

Design of highly continuous variable near-infrared vacuum squeezer

JIANFENG TIAN*, TENGFEI MENG, YAOLYAO ZHOU

Department of Physics, Taiyuan Normal University, Taiyuan 030619, China

Based on the below threshold parametric down-conversion process in the optical parametric oscillator (OPO), the simple and practical theoretical model for optimal designing a high efficiency continuous variable near-infrared vacuum squeezer is well established. Various limiting effects, such as optical losses, nonlinear conversion efficiency, and pump light absorption-induced temperature fluctuations, are taken into account to derive the geometry of the resonant cavity providing the optimal performance.

(Received December 11, 2020; accepted April 7, 2021)

Keywords: OPO, Continuous variable squeezed vacuum, Thermal effects

1. Introduction

Squeezed light is envisioned to have many practical applications, including quantum networks, cryptography, quantum computation and gravitational wave (GW) detection [1-5]. Especially the squeezed light on the alkali metal atomic absorption line can be used in scientific research for the interaction between nonclassical light and atoms, such as quantum optical storage, generation of atomic ensembles entanglement and quantum metrology [6, 7]. Compared with bright squeezed light, squeezed vacuum have a better nonclassical noise reduction at the wideband frequency range (Hz~MHz) [8, 9]. At present, the below threshold OPO belongs to the most successful approach of squeezed vacuum generation. To increase the sensitivity and fidelity as much as possible, it becomes more and more important to obtain a higher level squeezed light in practice [10]. In 2016, Vahlbruch *et al.* obtained quantum noise reduction of 15 dB at 1064 nm experimentally [11]. Nevertheless, the levels of squeezing corresponding to the alkali metal atoms transition lines are low at present. Most of the alkali atomic lines are usually near-infrared, and their pump beam operate in blue even ultraviolet regime, which are at the cutoff wavelengths of many nonlinear optical crystals with high absorption coefficient [12]. Due to the serious absorption of the pump beam, the near-infrared squeezed light was not satisfactory. In 2007, Takeno *et al.* observed only 9 dB of vacuum squeezing at 860 nm, which was close to the Cs D2 line [13]. In 2009, Burks *et al.* obtained 3 dB of squeezing at a measurement frequency of 50 kHz at 852 nm [14]. In these works, light absorption-induced thermal effects significantly deteriorate OPO performance including the conversion efficiency, cavity servo performance, and beam

quality, so it must be taken into account in the experiments. Compared with the obtained squeezing at the longer wavelength, the generated near-infrared squeezing is urgently needed further improving the degree of squeezed light for specific physical quantity detection. So how to optimize a highly continuous variable near-infrared vacuum squeezer remains an important issue.

At present, the technique for the near-infrared OPO has been developed based on the nonlinear crystals placed in the enhancement cavity. In order to get the satisfying output performance, one need carefully resonant cavity-designed with the bow-tie ring and the standing wave cavities configuration [11]. Motivated by these developments as well as by a variety of practical applications in quantum physics, in this paper we present an optimal design theoretical model of the efficient near-infrared squeezer. The analysis shows that, owing to the tight focusing inside the crystal, the server light absorption induces obvious crystal temperature fluctuation, which makes it impossible to lock the cavity to the maximum of the squeezing, and the key point for improving the performance is to adopt the proper waist focusing inside the nonlinear crystal. The cavity eigenmode parameters are determined, and then the geometric parameters of the resonator can be calculated by the ABCD transfer matrix theory. Thus, the appropriate optical path and resonator parameters of the cavity are selected, which can satisfy the requirement of the optical stability and the thermal stability.

2. Theory

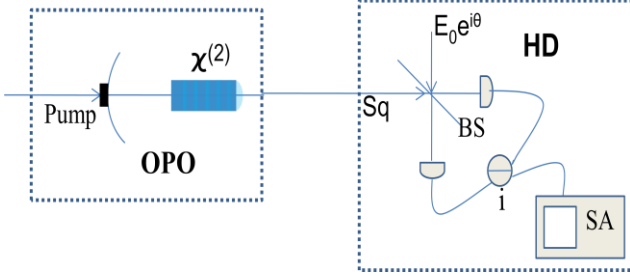


Fig. 1. Scheme used to derive the OPO squeezing spectrum observed in balanced homodyne detection (color online)

The basic components of OPO and homodyne detection setup are shown for reference in Fig. 1. The configuration of OPO to be considered is as follows: A nonlinear crystal characterized by second order susceptibility $\chi^{(2)}$ is contained in the resonant cavity formed by the mirrors, which is highly reflective at the probe beam frequency. The squeezed light are generated by degenerate parametric down conversion in a subthreshold OPO and emitted into the external reservoir. To measure the degree of squeezing of the output field from OPO, one can employ a balanced homodyne detection system (HD). The generated noise variances of the squeezed and antisqueezed quadrature are given as follows [13-15]:

$$V_{Asq, Sq} = 1 \pm \eta_{det} \eta_{esc} \frac{4x}{(1 \mp x)^2 + \Omega^2} \quad (1)$$

where $V_{Asq, Sq}$ are antisqueezing and squeezing levels,

$\Omega = \gamma / \Gamma$ is the normalized measurement frequency.

$x = \sqrt{P_2 / P_{2,t}}$ is the normalized nonlinear interaction

strength, P_2 is the pump power, and $P_{2,t}$ is the threshold pump power of OPO, and $P_{2,t} = (T + L_{loss})^2 / 4E_{NL}$, E_{NL} is the single pass nonlinear conversion coefficient. The detection

efficiency of the HD is given by $\eta_{det} = \eta_{tr} \times \eta_{vis}^2 \times \eta_{qu}$, and

includes the propagation efficiency η_{tr} , the interference

efficiency η_{vis}^2 and the quantum efficiency of the

photodiodes η_{qu} , where η_{vis} represents the quality of the

spatial mode overlapping between the signal and the local oscillator (LO) on the 50/50 beam splitter. η_{esc} is the

escape efficiency of OPO, which is defined as $\eta_{esc} = T / (T + L_{loss})$, T is transmittance of the output coupler mirror, L_{loss} is the OPO intracavity loss. The main factors which restrict the performance of OPO are: the single pass conversion efficiency, the intracavity loss and the available pump power.

The single pass conversion efficiency can be given by the well-known Boyd-Kleinman expression [16, 17]:

$$E_{NL} = \frac{4\omega^2 d_{eff}^2 L_C}{\epsilon_0 c^3 \lambda_\omega n_1 n_2} h(\alpha, \xi, \sigma) \exp[-(\alpha_1 + \alpha_2 / 2) L_C], \quad (2)$$

$$h(\alpha, \xi, \sigma) =$$

$$\frac{1}{2\xi} \int \int_{-\xi/2}^{+\xi/2} d\tau d\tau' \frac{\exp[-\alpha(\tau + \tau' + \xi) - i\sigma(\tau - \tau')]}{(1 + i\tau)(1 - i\tau')}, \quad (3)$$

where $\alpha = (\alpha_1 - \alpha_2) / 2b$, α_1 and α_2 are the linear absorption coefficients of the probe and the pump light.

$\xi = L_C / b$ is the focusing parameter, and $\sigma = \Delta k b$ is the

normalized wave-vector mismatch, which is given by

$$\Delta k = k_2 - 2k_1 - 2\pi / \Lambda, \quad b = k\omega^2, \quad \text{where } \Lambda \text{ and } \omega$$

represent the nonlinear crystal grating period and the Gaussian beam waist at the crystal center, respectively.

In the experiment process, pump light absorption induced any variations in crystal temperature cause the rotation of the squeezing angle and become a limitation to the measured squeezing level. The two dimensional steady state heat conduction equation inside the rectangular crystal is given by [18]:

$$K_x \frac{\partial^2 u(x, y, z)}{\partial x^2} + K_y \frac{\partial^2 u(x, y, z)}{\partial y^2} + q_v = 0 \quad (4)$$

where K is the thermal conductivity of the crystal, q_v is

the pump light absorption-induced heat source density.

When the pump Gaussian beam incident, the heat source density can be given by:

$$q_v = \frac{\alpha_2 P_2}{\pi \omega'(z)^2} \exp\left[-\frac{2(x^2 + y^2)}{\omega'(z)^2}\right] \exp(-\alpha_2 z) \quad (5)$$

$$\omega'(z) = \omega'_0 \sqrt{1 + \left(\frac{z}{z_0}\right)^2} \quad (6)$$

where $\omega'(z)$ is $1/e$ Gaussian radius of the pump beam,

ω'_0 represents the pump beam waist radius at the crystal

center, the beam Rayleigh length $z_0 = \pi\omega_0'^2 / \lambda_2$.

As described, OPO eigenmode parameters are determined, and then the geometric parameters of the resonator can be calculated by the ABCD transfer matrix theory for a Gaussian beam. For the resonant cavity configuration in Fig. 1, the eigenmode waist radius at the crystal center is given by [19]:

$$\omega_e = \sqrt{\frac{\lambda|B|}{\pi}} \left[1 - \frac{(D+A)^2}{4} \right]^{-\frac{1}{4}}, \quad (7)$$

as well as the resonant cavity stable operating condition:

$$S = |A+D|/2 \leq 1, \quad (8)$$

and the ABCD matrix can be expressed as:

$$\begin{aligned} \begin{bmatrix} A & B \\ C & D \end{bmatrix} &= \begin{bmatrix} 1 & l \\ 0 & 1 \end{bmatrix} \begin{bmatrix} 1 & 0 \\ 0 & \frac{1}{n} \end{bmatrix} \begin{bmatrix} 1 & l_2 \\ 0 & 1 \end{bmatrix} \begin{bmatrix} 1 & 0 \\ -\frac{2}{R_1} & 1 \end{bmatrix} \\ &\begin{bmatrix} 1 & l_2 \\ 0 & 1 \end{bmatrix} \begin{bmatrix} 1 & 0 \\ 0 & n \end{bmatrix} \begin{bmatrix} 1 & L_C \\ 0 & 1 \end{bmatrix} \begin{bmatrix} 1 & 0 \\ -\frac{2}{R_2} & 1 \end{bmatrix}, \end{aligned} \quad (9)$$

where l_2 is the direct distance between the crystal and the concave mirror whose curvature radius is R_1 . From the equations (7- 9), it shows that one can produce the desired waist by selecting cavity dimensions of L_C , R_1 , R_2 (the concave curvature radius of crystal) and l_2 .

3. Results and discussions

Firstly we examine the important limitations for the generation of strongly squeezed states in detail. The used data in calculations are $T=10\%$.

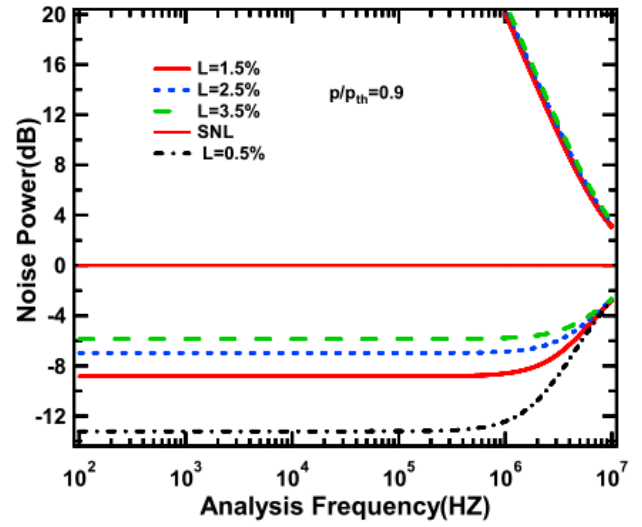


Fig. 2. Squeezing and antisqueezing amount as a function of measurement frequency for different intracavity losses, SNL: shot noise limit (color online)

High escape efficiency is necessary in order to generate stronger squeezing, which can be achieved by reducing the intracavity loss of OPO or increasing the transmittance of the output mirror. In the actual experimental system, however, high transmission rate is at the expense of much larger OPO threshold. Therefore, if the high squeezed degree is obtained by increasing the escape efficiency, the internal cavity loss of the resonator should be considered as much as possible. Fig. 2 shows the detected squeezing and antisqueezing amount as functions of measurement frequency for different intracavity losses, and $E_{NL}=2\% W^{-1}$. From the graph, we can see that the influence of the internal cavity loss on the squeezing level is more obvious than that on the antisqueezing quantum noise, even small loss can lead to an obvious degradation of the squeezing level. With the increasement of cavity losses, the degree of squeezing decreases dramatically. The intracavity loss mainly means linear loss, including the imperfect crystal coating, and the light absorption and scattering of the mirror. So one can employ semi-monolithic cavity configuration with lower intracavity linear loss and highly controllable as well as stable, as shown in Fig. 1.

Fig. 3 shows how the single pass conversion efficiency affects the quantum noise for various measurement frequencies, and $L_{loss}=0.5\%$. It can be seen that, the single pass conversion efficiency has a similar effect on the squeezing and the antisqueezing degree at the different measurement frequencies, and the obtained squeezing level will change significantly as the value of E_{NL} continues to increase without thermal effects. For the single pass conversion efficiency, from Eq. (2), it can be

seen that E_{NL} is a function of the effective nonlinear optical coefficient d_{eff} , the crystal length L_C , and the focusing of the probe light, i.e. ω , the value of the waist at the center of the crystal, a parameter that in turn is also determined by the geometry of the cavity (curvature radius of the mirrors and optical length of the cavity). We have shown E_{NL} as a function of the beam waist radius in Fig. 4 (black solid line). The parameters used here are $n_1 = 1.84$, $n_2 = 1.94$, $\alpha_1 \approx 1\% \text{ cm}^{-1}$, $\alpha_2 \approx 10\% \text{ cm}^{-1}$. The results show that the “optimal” focusing waist is $23\mu\text{m}$, and this corresponds to the theoretical values of $E_{NL}=4.2\% \text{ W}^{-1}$.

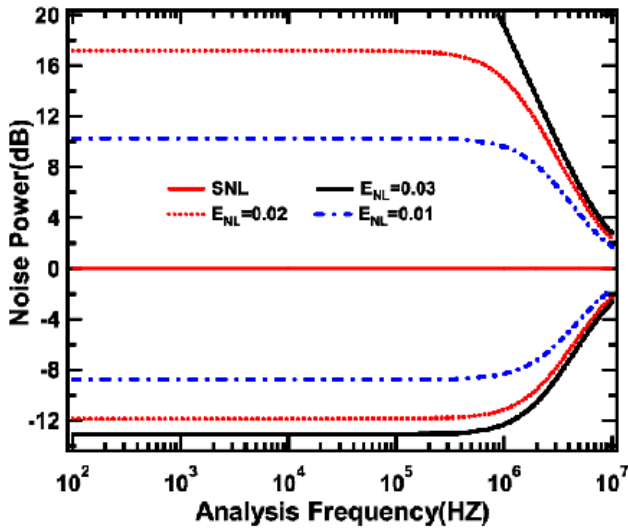


Fig. 3. Squeezing and antisqueezing amount as a function of measurement frequency for different single pass conversion efficiency. SNL: shot noise limit (color online)

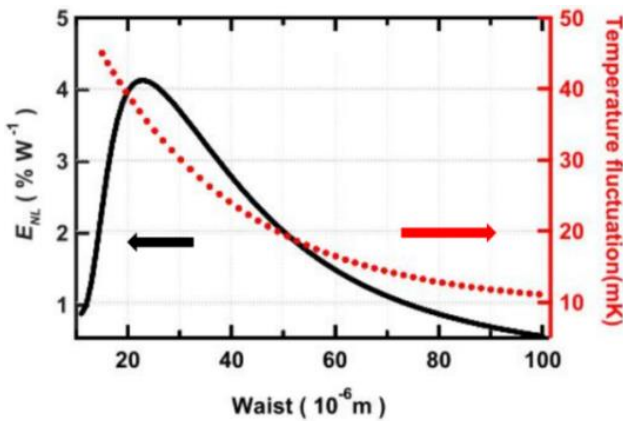


Fig. 4. Single pass conversion efficiency (black solid line) and temperature maximum fluctuation (red dotted line) versus OPO eigenmode waist radius (color online)

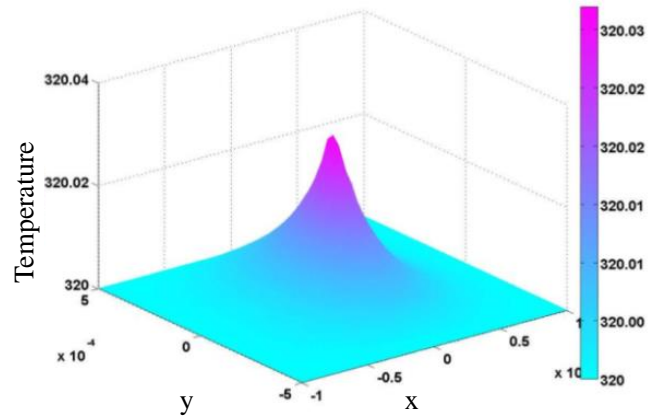


Fig. 5. Temperature distribution within the crystal central cross section, OPO eigenmode waist radius is $25\mu\text{m}$ (color online)

According to Eq. (4-6), we calculate and display the temperature distribution situations of the crystal, the initial phase matching temperature of the crystal is equal to 320K . Fig. 5 show the temperature distributions within the crystal central cross section, the corresponding eigenmode waist radius of OPO is $25\mu\text{m}$. It can be seen from the figure that the maximum temperature fluctuation of the crystal central cross section increases about 35mK . And then, we calculate maximum temperature fluctuation versus OPO eigenmode waist radius (red dotted line in Fig. 4). The result shows that the maximum temperature fluctuation changes significant with the various beam waist focusing. The smaller the waist radius is, the more serious the temperature fluctuation is. This is because the pump beam absorption increases with the rise of the incident pump light power density. On the one hand, if the crystal central temperature is too high, a large temperature difference will be formed inside the crystal, which will be harmful to the crystal. Fluctuation in the crystal temperature leads to a certain distribution of the refractive index and the crystal length, which results in the squeezed quadrature phase noise. On the other hand, the severe light absorption-induced thermal effects form a thermal gradient inside the crystal, which changes the eigenmode of OPO and then results in reduction of the interference efficiency of HD. In sum, when the focusing waist is too tight, such as the “optimal” focusing waist of $23\mu\text{m}$ mentioned above, it can increase the crystal thermal effect due to residual absorption, which will result in a lower squeezing level. The results tell that it is necessary to choose the proper cavity waist for high conversion efficiency. Based on this, we should choose a cavity waist of more than $45\mu\text{m}$ at the center of the crystal in practice.

At present, the favorable nonlinear crystal used in the experiment is usually PPKTP, due to a large nonlinear coefficient, absence of walk-off, and no BLIIRA. As determined by the ABCD matrix method for Gaussian beams, the crystal center waist radius is more than $45\mu\text{m}$. According to the equations (7-9), Fig. 6 shows that cavity eigenmode waist radius and the cavity stability varies with

the distance between the crystal and the concave mirror with different concave curvature radius R_1 and R_2 . When the PPKTP crystal length is 10 mm, and the curvature radius R_2 is 10, 15 and 20 mm, the corresponding results are shown in the figure. For different curvature radius R_1 of the plane-concave (20 mm, 25 mm, and 30 mm), we can get the approximately same waist radius by choosing the cavity length l_2 . The figure shows that our well-designed cavity always remains the stability region and the eigenmode waist radius will not change very much, even if the cavity length change a few millimeters in the actual operation process, which can improve the stability of the output.

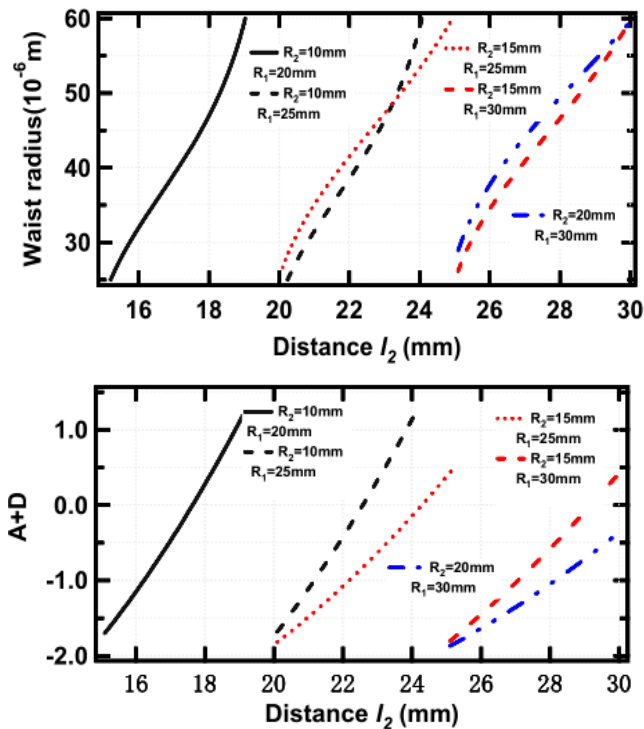


Fig. 6. The cavity eigenmode waist radius and stability varies with the length l_2 (color online)

4. Conclusion

In conclusion, we have presented the theoretical optimal design model of the efficient and stable near-infrared squeezer resonator cavity. Firstly, in order to reduce the loss of OPO, one need employ a semi-monolithic standing wave cavity configuration with lower intracavity loss and fine controllability as well as mechanical stability. Owing to the tight focusing inside the crystal, the server light-absorption induces obvious crystal temperature fluctuation, and the key point for improving the performance is to adopt the proper waist focusing in the nonlinear crystal. The results show that one should utilize OPO eigenmode waist radius of more than $45 \mu\text{m}$ in practice. The cavity eigenmode parameters are determined, and then the geometric parameters of the resonator can be calculated by the ABCD transfer matrix theory. Thus, the

appropriate optical path and resonator parameters of the cavity are selected, which satisfied the requirement of the optical stability and the thermal stability.

Acknowledgments

This work was supported by the Natural Science Foundation of Shanxi Province of China (Grant No. 201901D111293).

References

- [1] E. S. Polzik, J. Carri, H. J. Kimble, Phys. Rev. Lett. **68**, 3020 (1992).
- [2] L. Hesselink, S. S. Orlov, A. Liu, A. Akella, D. Lande, R. R. Neurgaonkar, Science **282**, 1089 (1998).
- [3] H. Dittlbacher, B. Lamprecht, A. Leitner, F. R. Aussenegg, F. R. Aussenegg, Opt. Lett. **25**, 563 (2000).
- [4] J. Alnis, U. Gustafsson, G. Somesfalean, S. Svanberg, Appl. Phys. Lett. **76**, 1234 (2000).
- [5] X. J. Zuo, Z. H. Yan, Y. N. Feng, J. X. Ma, X. J. Jia, C. D. Xie, K. C. Peng, Phys. Rev. Lett. **124**, 173602 (2020).
- [6] S. Suzuki, H. Yonezawa, F. Kannari, M. Sasaki, A. Furusawa, Appl. Phys. Lett. **89**, 061116 (2006).
- [7] J. Hald, J. L. Sørensen, C. Schori, E. S. Polzik, Phys. Rev. Lett. **83**, 1319 (1999).
- [8] J. R. Wang, Q. W. Wang, L. Tian, J. Su, Y. H. Zheng, Chin. Phys. B **29**, 034205 (2020).
- [9] T. Eberle, S. Steinlechner, J. Bauchrowitz, V. Händchen, H. Vahlbruch, M. Mehmet, H. Müller-Ebhardt, R. Schnabel, Phys. Rev. Lett. **104**, 251102 (2010).
- [10] X. C. Sun, Y. J. Wang, L. Tian, Y. H. Zheng, K. C. Peng, Chin. Opt. Lett. **17**, 072701 (2019).
- [11] H. Vahlbruch, M. Mehmet, K. Danzmann, R. Schnabel, Phys. Rev. Lett. **117**, 110801 (2016).
- [12] F. Villa, A. Chiummo, E. Giacobino, A. Bramati, J. Opt. Soc. Am. B **24**, 576 (2007).
- [13] Y. S. Takeno, M. Yukawa, H. Yonezawa, A. Furusawa, Opt. Express **15**, 4321 (2007).
- [14] S. Burks, J. Ortalo, A. Chiummo, X. Jia, F. Villa, A. Bramati, J. Laurat, E. Giacobino, Opt. Express **17**, 3777 (2009).
- [15] W. H. Yang, S. P. Shi, Y. J. Wang, W. G. Ma, Y. H. Zheng, K. C. Peng, Opt. Lett. **42**, 4553 (2017).
- [16] G. D. Boyd, D. A. Kleinman, J. Appl. Phys. **39**, 3597 (1968).
- [17] J. F. Tian, C. Yang, J. Xue, Y. C. Zhang, G. Li, T. C. Zhang, J. Opt. **18**, 055506 (2016).
- [18] J. L. Liu, X. Y. Chen, Y. J. Yu, C. T. Wu, F. Bai, G. Y. Jin, Phys. Rev. A **93**, 013854 (2016).
- [19] A. E. Siegman, 1986, Lasers (Mill Valley, CA: University Science Books).

*Corresponding author: tianjf@tynu.edu.cn